Desalination and Water Treatment
www.deswater.com
doi: 10.5004/dwt.2023.29500

292 (2023) 97–107
April

Removal of lead metal from groundwater using graphene oxide nanosheet functionalized with ethylenediaminetetraacetic acid

R.A. Rayan, Waleed F. Khalil*, M.A. Sadek

Nuclear and Radiological Safety Research Center (NRSRC). Egyptian Atomic Energy Authority (EAEA),
emails: waleed_fekry12878@yahoo.com (W.F. Khalil), rafatrayan@yahoo.com (R.A. Rayan), m.sadek499@yahoo.com (M.A. Sadek)

Received 14 September 2022; Accepted 27 March 2023

ABSTRACT

One of the important carbon materials, graphene oxide (GO), has several oxygen-containing functional groups in the form of epoxy, hydroxyl, and carboxyl on its basal plane and its edges. Due to its unique structure, it has attracted increasing interest in multidisciplinary studies of physical and chemical attributes. GO-based compounds in particular are potential for environmental uses in energy and clean-up. In the present work, GO was functionalized with ethylenediaminetetraacetic acid (EDTA) to remove lead ions from water. The as-prepared and EDTA functionalized GO were applied as adsorbents to remove Pb(II) from groundwater in Western El-Mina area, mid Upper Egypt. The adsorption of lead under effects of contact time, temperature and pH has been investigated. It is concluded that the maximum adsorption capacity of pure GO for the lead was about 246 mg/g while that of GO-EDTA was about 360 mg/g. It is indicated that pH~6 and temperature ~40°C are the best conditions for Pb(II) removal from water. The adsorption experimental data was evaluated through elucidating the adsorption kinetic using pseudo-first-order and pseudo-second-order. It is revealed that the pseudo-second-order model is the best representing adsorption kinetics model for both GO and GO-EDTA. Additionally, the equilibrium adsorption isotherm has been studied using the Langmuir and Freundlich isotherms models. The adsorption equilibrium isotherms data followed the Langmuir model better than the Freundlich model. The present work indicated that the prepared materials (GO and GO-EDTA) are efficient adsorbents for lead removal.

Keywords: Pb(II); Graphene oxide; Ethylenediaminetetraacetic acid; Water treatment

1. Introduction

Water is currently one of the most essential resources and it has economic, social, political, and environmental importance worldwide. In recent years, water pollution has become a severe environmental issue that has gained worldwide attention, especially as a result of the fast industrial development that has led to the introduction of numerous pollutants into aquatic systems [1]. Metals, dyes, biodegradable waste, phosphates and nitrates, heat, silt, fluoride, hazardous and toxic compounds, radioactive pollutants, pharmaceuticals, and personal care items are pollutants of main concern. To maintain the environmental quality and health safety, different metal pollutants should be removed from wastewater and water resources before it is released into the environment. The complete removal of heavy metals and organic contaminants from natural water resources not only protects the environment, but also prevents hazardous contaminants transfer in food chains [2]. Because of the chemical and physical properties of lead such as high malleability, low melting point, ductility, and resistance to corrosion, it is one of the most common heavy-metals widely used for industrial applications such as storage batteries, alloys, cable sheaths, solder, X-ray equipment, radiation

* Corresponding author.

shielding, plastics, paint, automobiles, ceramics, gasoline as antiknock agent and pesticides industries, which have led to environmental and health problems [3–7]. The World Health Organization (WHO) and the United States Environmental Protection Agency (USEPA) have determined recommended maximum values for lead(II) in drinking water at 10 and 15 ug/L, respectively. Lead is non-biodegradable material and it tends to accumulate in blood, soft tissues, and bones. Consumption of water containing Pb(II), even at low concentrations, can cause many chronic or acute diseases in humans, including brain damage, gastrointestinal distress, kidney damage, mental retardation, developmental delays, behavior problems, mental and physical disorders, as well as decreased cognitive function, inattention, and impulsivity in children at blood lead levels [8,9]. Therefore, it's critical to develop innovative techniques for efficiently identifying and removing lead(II) from wastewater [10]. Because of the high levels of lead in waste effluents, each country's regulatory body may be required to strictly adhere to discharge and exposure regulations. For the selective detection and removal of Pb(II) ions from environmental, industrial, food, and biological samples, the development of a novel material is always essential [9]. Remediation by adsorption offers; low cost, reusability, easiness and low sludge production, due to the adsorption process is deemed more important than other traditional wastewater treatments such as electrochemical, membrane processes, chemical precipitation, evaporation, and filtration for the removal of heavy metals [11].

Compared to conventional adsorbents, which have a limited adsorption capacity, nanomaterials such as nanoscale zero-valent iron [11], nanoscale organo-functionalized SiO_2-Al_2O_3 [12], aluminum–silicate nanoparticles [13] and graphene oxide (GO) [2] could provide effective absorbance for efficiently eliminating metal contaminants from wastewater. The increased surface-to-volume ratio of nanomaterials renders them more reactive. These molecules excite experts, who use them to remove heavy metals and radioactive materials from wastewater [14]. Due to its high specific surface area and the addition of functional groups such as hydroxyl, carboxyl, and epoxy on the sheet edges, GO provides superior metal ion adsorption properties [15,16]. Due to its large theoretical specific surface area, GO is a promising to be modified and applied in the future as a more effective adsorbent for the removal of various water pollutants. These protruding oxygen groups can serve as anchoring sites for attaching ions electrostatically and/or coordinately, particularly for metals with differing valence states [17–20]. The functionalization of the graphene oxide surface with ethylenediaminetetraacetic acid (EDTA) was demonstrated by Madadrang et al. [2] by the use of the silanization method. Therefore, this showed a significant improvement in the adsorption capacity for the adsorption of hazardous heavy metals from aqueous solution, such as Pb(II), Cu(II), Ni(II), and Cd(II). EDTA-GO has the potential to be an excellent adsorbent due to the presence of both OH and COOH groups on its surface in addition to the EDTA. Madadrang et al. [2] reported that EDTA-modification highly increases the adsorption capacity of GO due to ethylenediaminetetraacetic acid's chelating activity. Moreover, they indicated that EDTA-GO could be reused after being washed with HCl and proved that EDTA-GO was an excellent adsorbent for the elimination of hazardous heavy metals with potential uses in environmental clean-up [2]. It could be concluded that the GO-EDTA is an ideal adsorbent for heavy metals. where EDTA is linked to substrate, it forms a stable chelate with metal ions, the introduction of EDTA groups to the GO surface can significantly increase the adsorption capacity of GO [2].

In the present work, the GO surface have been successfully functioned using EDTA. The X-ray diffraction (XRD) and transmission electron microscopy (TEM) techniques were used for studying the crystalline structure and morphology of GO, the Fourier-transform infrared spectroscopy (FT-IR) technique was used to compare GO before and after EDTA functionalization. GO and GO-EDTA were examined as potential adsorbents for Pb(II) removal from water. In the adsorption process, the effects of contact time, metal concentration, pH, and temperature were examined. The present work has been conducted on groundwater samples collected from the Eocene and quaternary aquifers in a pilot-areas allocated for agriculture expansion in the desert reach in mid-Upper Egypt. The current work highlights the water quality perspective in irrigation and other uses.

2. Experimental

2.1. Materials

The following materials were used in the present work: graphite powder, potassium permanganate ($KMnO_4$), sulfuric acid (H_2SO_4, 98%), phosphoric acid (H_3PO_4, 85%), hydrogen peroxide (H_2O_2, 30%), hydrochloric acid (HCl, 36.5%), EDTA, ethanol, methanol, and lead nitrate ($PbNO_3$). The indicated materials were all used at analytical grade and did not need any additional purification. Deionized water was utilized in all experiments.

2.2. Graphene oxide preparation

Graphene oxide was prepared from graphite powder using improved Hummers' method [21,22]. The following steps were followed for GO oxidation: (a) in ice path (temperature <0), graphite was strongly oxidized using mixture (v/v) of concentrated H_2SO_4 and H_3PO_4 (2:1) under vigorous stirring followed by slow addition of $KMnO_4$ (18 g/3 g graphite) to the suspended mixture. (b) The oxidized GO suspension was poured on iced water containing H_2O_2 (30 wt.%) and exfoliated in water by ultrasonic wave. (c) GO was washed several times using HCl 10% and deionized water through centrifugation. (d) The resultant GO was dried under vacuum at 60°C [14,23,24].

2.3. Preparation of GO-EDTA

According to Khalil et al. [25], GO was functionalized with EDTA. In a 1,000-mL flask, 0.8 g of produced graphene oxide was dissolved in 400 mL of methanol and sonicated for 120 min. After combining the graphene oxide suspension with 8.68 g of EDTA, it was refluxed at 60°C for 16 h. The addition of 200 mL of methanol eliminated all the unreacted compounds. The product of 1 h of centrifugation at 10,000 rpm was separated with multiple washes of filtered

water and methanol. The prepared sample was dried in a 60°C vacuum oven for 12 h [26–29].

2.4. Characterization

In order to characterize the FT-IR spectra of GO, EDTA, and GO-EDTA with an FT-IR spectrometer, the KBr pellets technique was utilized (Shimadzu 8400, Japan). It was decided to study each spectrum using an X-ray diffractometer (PANalytical Empyrean, Netherlands) and CuK radiation (wavelength = 1.54045) so that the interaction between graphite and graphene oxide could be comprehended more thoroughly. The TEM was utilized in this work (JEOL JEM-2100, Japan). The Zeiss EVO MA10 scanning electron microscope was used explore the surface morphology.

2.5. Batch adsorption experiments

Using the batch method and 120 mL polyethylene caps, the following adsorption experiments were conducted. All adsorption tests utilized a stock solution of 0.5 g of GO or GO-EDTA (adsorbent) suspended in 1.0 L of deionized water. The adsorbate stock solution was made by dissolving $Pb(NO)_3$ in 1.0 L of deionized water. Then, it was diluted to form lead solutions with concentrations of 25, 50, 100, and 250 ppm (II). Adjusting the pH was done by adding HCl (0.1 N) or NaOH (0.1 N). Then, various amounts of the adsorbent were applied, with the total volume of each experiment being constant at 100 mL. The adsorption suspension was shaken at 200 rpm for 4 h.

Using gold nanoparticles (GNP) and a colorimetric technique, the concentration of lead was measured. According to Ding et al. [30], GNPs reacted with lead metal to produce a color change that can be detected using a spectrophotometer at 650 nm; the peak intensity of absorption intensity was related to the Pb(II) concentration.

The amount of lead adsorbed on GO or GO-EDTA was determined by subtracting the initial concentration (C_o) from the equilibrium concentration (C_e). The adsorption performance was quantified in terms of adsorption percentage (%) and adsorption capacity, which were determined using the following equations:

$$\text{Uptake removal } \% = \frac{C_o - C_e}{C_o} \times 100\% \quad (1)$$

$$\text{Adsorption capacity} = \frac{\left(C_o - C_e\right)V}{m} \quad (2)$$

where C_o (mg/L) and C_e (mg/L) are for initial and equilibrium concentrations of lead. V (mL) represents the volume of the suspension, and m (g) is the weight of the adsorbent. The experimental data are all averages of the triplicate determinations.

2.6. Removal of lead ions from real groundwater samples

The application of GO-EDTA nanosheets for removing Pb(II) ions from real water was explored and investigated by collecting seven groundwater samples from Western El-Mina area Upper Egypt (Fig. 1.) depending on an increased level of lead in the selected samples. A 500 mL sample of the selected water samples was mixed with 250 mg of GO-EDTA and shaken for 2 h at room temperature. A 15 mL mixing solution was taken in a falcon tube and centrifuged for 30 min at 5,000 rpm. The supernatant was separated and the level of lead ions measured.

3. Results and discussion

3.1. Characterization of GO and GO-EDTA

The high-resolution transmission electron microscopy (HR-TEM) and scanning electron microscopy imaging of graphene oxide is shown in Fig. 2. The layered structure of graphene oxide has been seen to have a surface that is both flat and transparent, with some folding and wrinkling. Before and after the graphite oxidation operations, the XRD analysis was performed on graphite powder. Fig. 3a displays a sharp peak at 2θ = 26.1695° associated with graphite powder with *d*-spacing = 3.34. After graphite layers were oxidized, the graphite peak disappeared, and a new graphene oxide peak at 2θ = 10.93° was formed. Additionally, function groups were inserted between graphite layers to increase the *d*-spacing value to 8.0427. This demonstrated that graphite experienced significant oxidation during the formation of graphene oxide. These results are highly consistent with previous researches [31–33]. Raman spectroscopy is very useful tool for characterizing GO. The spectra results of Raman are shown in Fig. 3b. The recorded Raman spectroscopy of GO shows the appearance of two major bands D-band at 1,345 cm^{-1} and G-band at 1,597 cm^{-1}. The D and G bands intensity ratio (I_D/I_G) was 0.842. These results completely agree with the previously published work [34].

Fig. 4, presents the FT-IR spectra of both GO and an EDTA-modified version of GO. The FT-IR spectra of GO reveal peaks at 1,080; 1,155; 1,228; 1,286; 1,639; 1,734 and 3,431 cm^{-1}. These peaks are presented as various oxygen-containing functional groups and corresponded to the stretching vibrations of C–O, C–OH, C=O, C–C, C=C, COOH, and O–H bonds, respectively. After loading EDTA onto the surface of

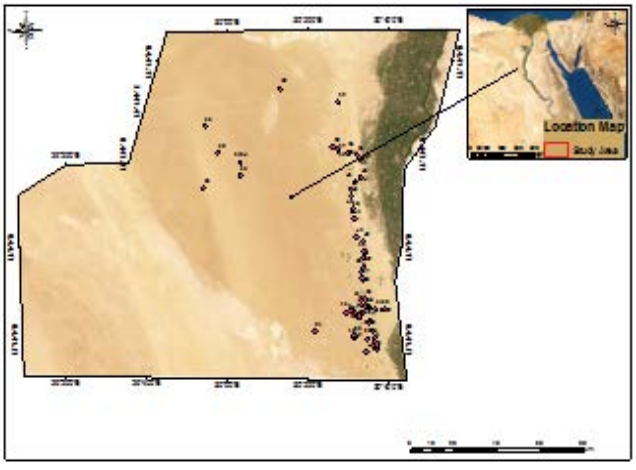

Fig. 1. Location of collecting groundwater samples from Western El-Mina area Upper Egypt.

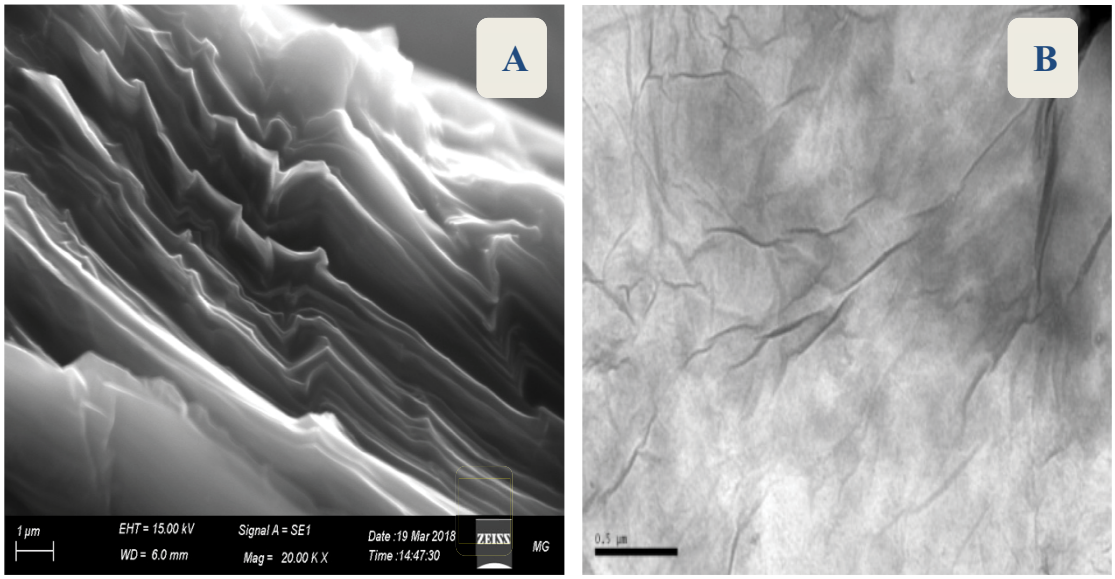

Fig. 2. (a) Scanning electron microscopy image of graphene oxide and (b) high-resolution transmission electron microscopy image of GO.

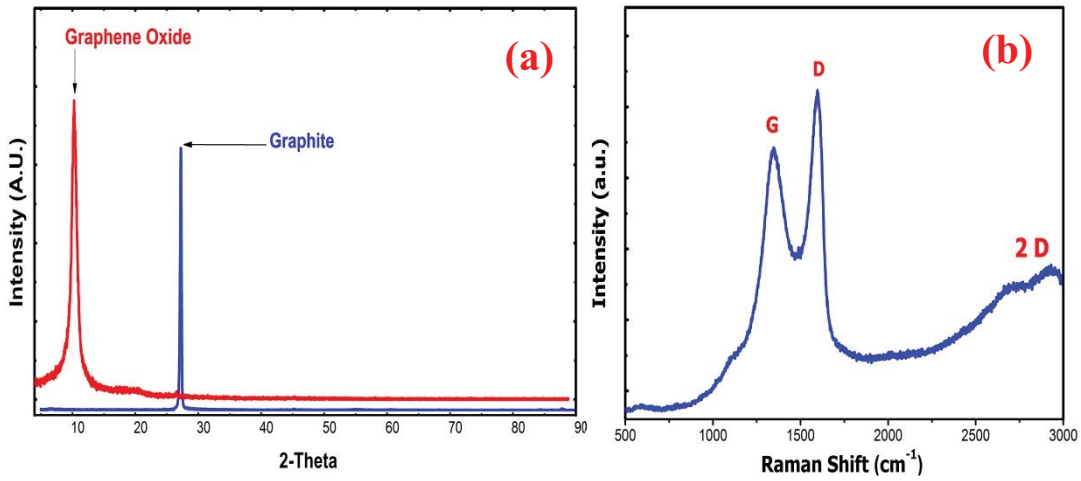

Fig. 3. (a) X-ray diffraction patterns of graphite and GO and (b) Raman spectra of GO.

graphene oxide, the O–H stretching appeared at 3,173 cm^{-1}, which may be attributed to the N–H stretching vibrations in the spectrum of EDTA. Additionally, a new peak was observed at 1,392 cm^{-1}, which can be illustrated to the C–N stretching of the EDTA molecule. The FT-IR spectrum produced an evidence that the EDTA was loaded onto the surface of the graphene oxide in an efficient way [2,26].

3.2. Adsorption studies

3.2.1. Effect of adsorbate concentration

The adsorption capacities for a 0.5 g/L adsorbent were investigated by applying different concentrations of lead (25, 50, 100, and 250 ppm) while maintaining a pH value of 6 and a temperature of 25°C. As shown in Fig. 5, by increasing the concentration of the adsorbate from 25, 50, 100 to 250 ppm, the adsorption capacity of GO to lead increased from 49.8, 92.8, 180 to 246 mg/g, but the adsorption capacity of GO-EDTA increased from 49.8, 99.4, 198 to 360 mg/g. Because of the increased number of metal ions that are vying for the active sites of GO and GO-EDTA, the adsorption capacity of GO and GO-EDTA increases as lead concentration increases. This is owing to the fact that GO and GO-EDTA have more active sites available. As the concentration of these metal cations rises, the driving power of the concentration gradient will experience an accompanying rise as well. After an initial period of fast expansion, the extent of adsorption at various concentrations continues to rapidly decrease as the adsorption process continues, eventually leading to equilibrium. This is because there are a large number of vacant active sites on the surface of the GO

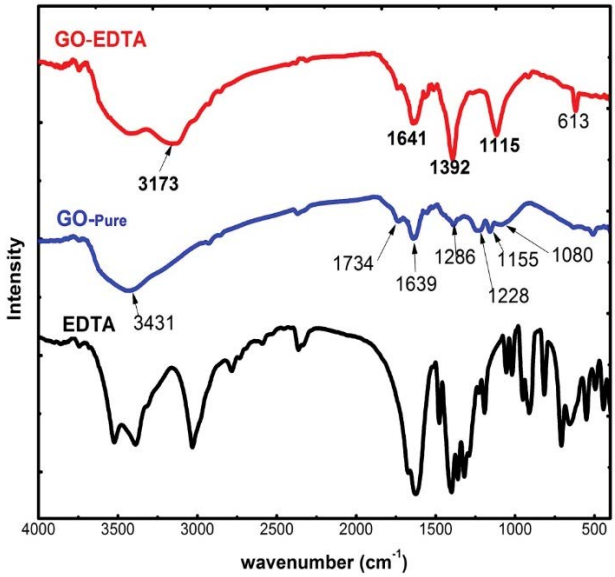

Fig. 4. Fourier-transform infrared spectra of GO, EDTA and GO modified with EDTA.

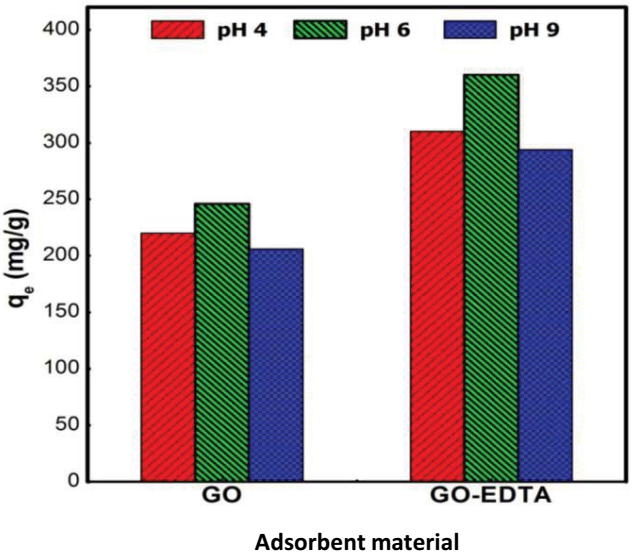

Fig. 6. Effect of pH on adsorption capacity of lead ions for pure GO and GO-EDTA at pH 4, 6 and 9.

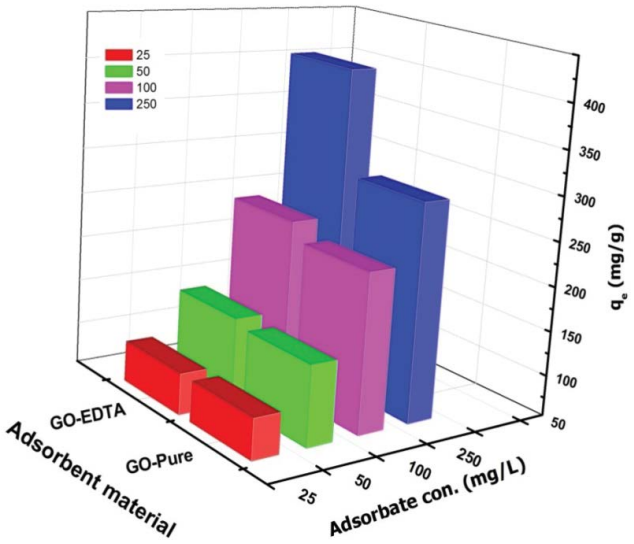

Fig. 5. Effect of metal ion concentration for GO pure and with GO-EDTA.

that are available for adsorption during the primary stage. However, once a certain amount of time has passed, it is difficult for the remaining vacant sites to be occupied.

3.2.2. Effect of pH

The pH value of the solution is a major factor in the adsorption of lead ions because it affects the surface charge of graphene oxide. The removal of lead ions from water as a function of solution pH is displayed in Fig. 6. As shown, the removal of lead ions was low in an acid media. This could be due to the fact that the surface functional groups of GO-EDTA have been protonated, producing repulsion interactions between the lead ions. When the pH value rose from 4 to 6, the elimination of Pb(II) ions increased rapidly from 310 to 360 mg/g. while nearly complete lead removal was observed at pH = 6. By increasing the pH value of GO and GO-EDTA, the surface becomes more deprotonated, hence raising Pb(II) adsorption. However, the adsorption capacity reduced to 294 mg/g when the pH value increased to 9. The negatively charged surface and the formation of strong interactions between the present OH ions on the surface of GO and GO-EDTA resulted in a constant decrease in the removal efficiency of lead ions. This is due to the creation of a combination between graphene oxide sheet and lead ions, which restricted the ions' adsorption. In addition, unbound Pb(II) ions can precipitate and form $Pb(OH)_2$ at higher pH values.

3.2.3. Effect of temperature

From 25°C to 40°C, the temperature's impact on the adsorption capacity of GO and GO-EDTA was investigated (Fig. 7). As the temperature increased, the capacity to remove lead ions from water increased from 360 to 390 mg/g. The increased adsorption capacity indicates that the adsorption process is endothermic. In general, the adsorption capability decreases as the heat increases to 60°C. The decrease in adsorption as the temperature increases indicates that adsorption is exothermic.

3.3. Adsorption isotherms

The association between various concentrations of lead ions (25, 50, 100, and 250 ppm) on pure GO and GO-EDTA as absorbents and in equilibrium was examined using an adsorption isotherm. On the surface of the adsorbent, the connection between the equilibrium concentration (C_e) and the uptake at equilibrium (q_e) for lead ions is illustrated in Fig. 8. As observed, an increase in the concentration of Pb(II)

solution was accompanied by an increase in the adsorption capacity of Pb(II). At a concentration of 250 ppm, the sorption capacity of GO-EDTA reached its highest limit, whereas the capacity of pure GO was at its lowest limit. When GO was functionalized with EDTA, this produces a larger surface area and increases functional groups which enabled the rapid sorption of Pb(II), which is a possible explanation for the observed phenomenon.

3.3.1. Freundlich and Langmuir

The adsorption equilibrium data were analyzed in terms of Freundlich and Langmuir adsorption isotherms for the equilibrium data obtained at pH~6 and temperature = 25°C. Adsorption isotherms are mathematical models which are most commonly used to describe the distribution of the adsorbate species between liquid and adsorbent. In the Langmuir adsorption model, it is assumed that the highest adsorption is related to a saturated monolayer of solute molecules on the surface of the adsorbent, and there are no cross interactions between the adsorbed materials [35]. The linear form of Langmuir isotherm is given by the following equation:

$$\frac{C_e}{q_e} = \frac{1}{q_{\max} K_L} + \frac{1}{q_{\max}} \tag{3}$$

where C_e (mg/L) is the equilibrium concentration, q_e (mg/g) is the amount of adsorbate adsorbed per unit mass of adsorbent at equilibrium, $q_{\max}$ is maximum adsorption capacity (mg/g) and K_L is the Langmuir adsorption constant (mg/L).

When C_e/q_e was plotted vs. C_e, a linear fitness of the data has been obtained, its slope and intercept equal $1/q_{\max}$ and $1/q_{\max} K_L$. Fig. 9 and Table 1 show that the maximum adsorption capacities of GO and GO-EDTA for lead are 252.5 and 363.0 mg/g, respectively. The K_L values were found to be 0.279 and 1.432 for lead on the GO and GO-EDTA, respectively, on the other hand the R^2 values were more than 0.999.

The Freundlich isotherm is applied to multilayered adsorption and adsorption on a heterogeneous surface. It is given by the following equation:

$$\ln q_e = K_F + \frac{1}{n} \ln q_e \tag{4}$$

where q_e is the amount of adsorbate ion per unit mass of adsorbent (mg/g), C_e is the concentration of ions in solution at equilibrium (mg/L), K_F is the Freundlich constant which is indicator of adsorption capacity ($mg^{(1-1/n)} \cdot L^{(1/n)}/g$) and n is the adsorption intensity. The slopes and intercepts of the linear Freundlich plots ($\ln q_e$ vs. $\ln C_e$) are used to calculate the Freundlich constants. The Freundlich plots of the Pb(II) on GO and GO-EDTA are shown in Fig. 10, and the values of Freundlich isotherm are listed in Table 1. The K_F values were found to be 4.885 and 3.725 for lead ion on the GO and GO-EDTA, respectively. While, n was found to be 4.03 and 3.678 for lead on the GO and GO-EDTA, respectively, the R^2 was 0.909 and 0.705. Comparing the correlation coefficients of the linear regressions (R^2) for Langmuir isotherm model

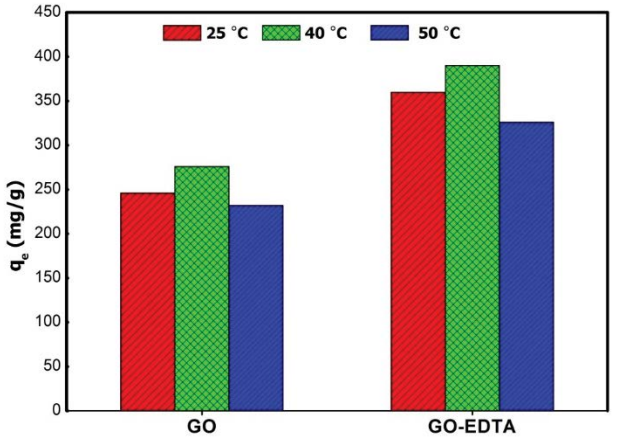

Fig. 7. Effect of temperature on adsorption capacity of lead for GO pure and GO-EDTA at pH 6.

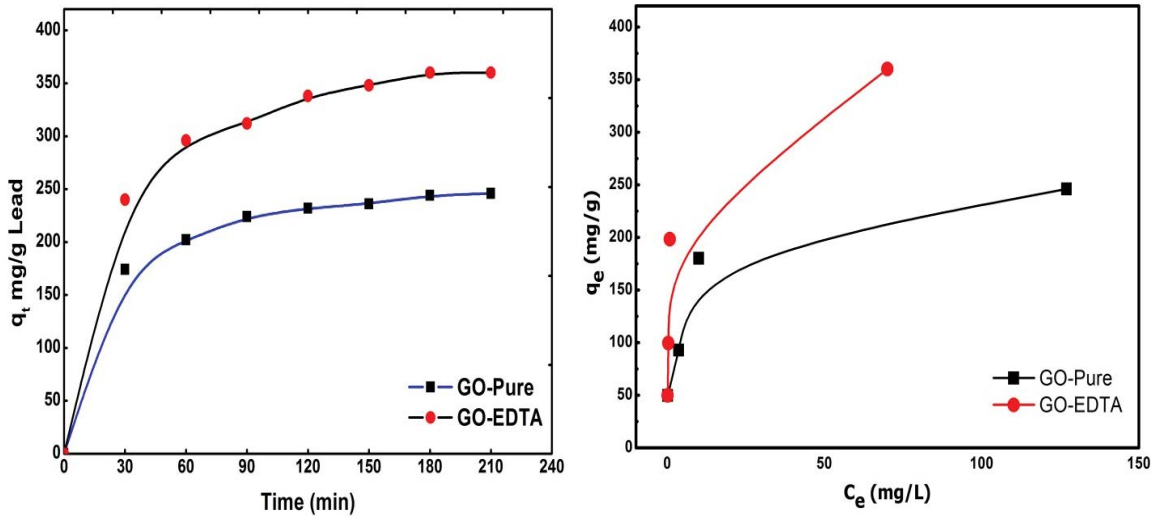

Fig. 8. Adsorption isotherm for lead onto GO and GO-EDTA.

to that of the Freundlich model in Table 1, it can be concluded that Langmuir model fit the adsorption equilibrium data better than the Freundlich model where it has higher R^2 values than 0.999) for both GO pure and GO-EDTA.

3.4. Adsorption kinetic studies

In present study, pseudo-first-order and pseudo-second-order were applied as kinetic models. The first-order rate equation is the earliest known to describe the adsorption rate based on adsorption capacity. The linear form of the first-order rate equation is as follows:

$$\ln\left(q_e - q_t\right) = \ln q_e - K_1 t \tag{5}$$

where q_e is the amount of ion adsorbed onto the adsorbent at equilibrium (mg/g), q_t is the amount of Pb(II) adsorbed onto the GO and GO-EDTA at any time t (mg/g), and K_1 (min^{-1}) is the rate constant of the pseudo-first-order adsorption which can be calculated from the slope of the linear plot of $\ln(q_e - q_t)$ vs. t (slope = K_1, q_e = exp intercept). Fig. 11a shows the first-order formation of its Pb(II) adsorption on GO and GO-EDTA, respectively. The results obtained are indicated in Table 2. The calculated q_e was equal to 115.2 and 217.15 mg/g for lead of GO and GO-EDTA as adsorbent, respectively. The kinetics of the second-order model is differentiated

Table 1
Langmuir and Freundlich adsorption constants associated to the adsorption isotherms of lead on GO pure and GO-EDTA

	Material		
Models	Parameters	GO pure	GO-EDTA
	q_{exp} (mg/g)	246.0	360.0
	q_{max} (mg/g)	252.5	363.6
Langmuir	K_L (mg/L)	0.279	1.432
	R^2	0.9978	0.9999
	K_F (mg/g (mg/L)n)	4.88563	3.72513
Freundlich	n	4.0399	3.6782
	R^2	0.90911	0.750

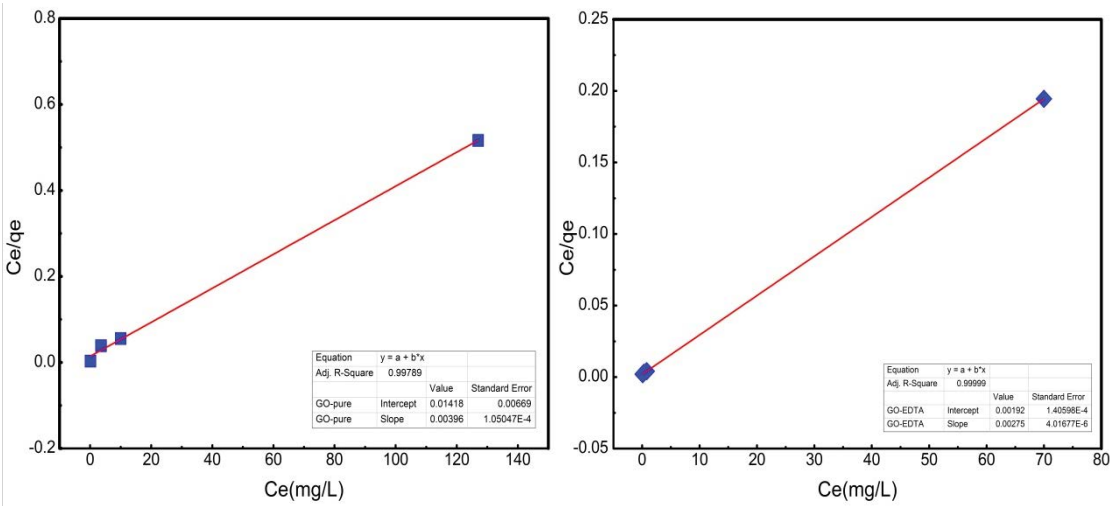

Fig. 9. (a) Langmuir isotherm for on pure graphene oxide and (b) graphene oxide with EDTA.

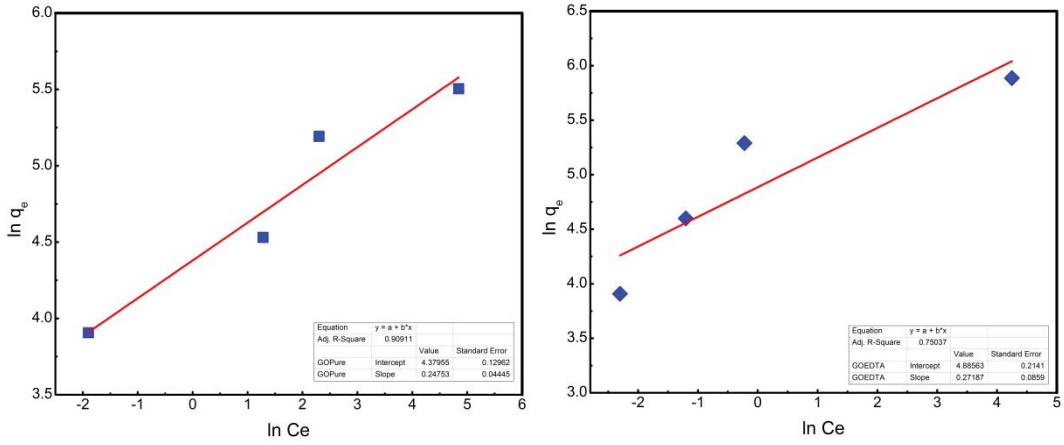

Fig. 10. Freundlich isotherm for lead ion adsorbed on to pure GO and GO-EDTA.

from solute concentration models based on adsorption concentration. The linearized form of the pseudo-second-order model as given by Ho [36] as follows:

$$\frac{t}{q_t} = \frac{1}{k_2 q_e^2} + \frac{1}{q_e} t \tag{6}$$

where K_2 (g/mg·min) is the rate constant of the pseudo-second-order adsorption and can be calculated from the slope and intercept of the plot of t/q_t against t. The results of second-order modeling are shown in Table 2 and Fig. 11b. The calculated q_e values were found to be 265.9 and 398.4 mg/g for lead on the GO and GO-EDTA, respectively. On the other hand, the coefficients of the correlation value (R^2), for the second-order kinetic model is between 0.998 and 0.9991. Comparing the q_e experimental with q_e calculated values, shows an acceptable match indicating that second-order kinetic model is the best representative for adsorption of lead on GO and GO-EDTA. Table 3 illustrated the comparison of the adsorption capacity of GO and GO-EDTA with other adsorbents. It can be concluded that the maximum adsorption capacity of GO-EDTA was higher than that of most of the other adsorbents, which was attributed to functional groups on the surfaces of GO-EDTA.

3.5. Stability and reusability

Previous research has shown that the GO and GO-EDTA adsorbents are reusable for lead removal. Azam et al. [37] investigated the GO adsorbent's ability for reuse following six cycles of regeneration with 0.1 M H_2SO_4. The result demonstrates that even after 6 repeated cycles, the GO

Table 2
Coefficients of pseudo-first-order, pseudo-second-order adsorption kinetic models Pb(II) = 250 mg/L, GO and GO-EDTA = 0.5 g/L at pH = 6

Models	Material		
	Parameters	GO pure	GO-EDTA
First-order	$q_{e,exp.}$ (mg/g)	246	360
	$q_{e,cal.}$ (mg/g)	115.2	217.15
	K_1	–0.01698	–0.01891
	R^2	0.98152	0.97991
Second-order	$q_{e,cal.}$ (mg/g)	265.9	398.4
	K_2	2.17×10^{-4}	1.18×10^{-4}
	R^2	0.99955	0.99899

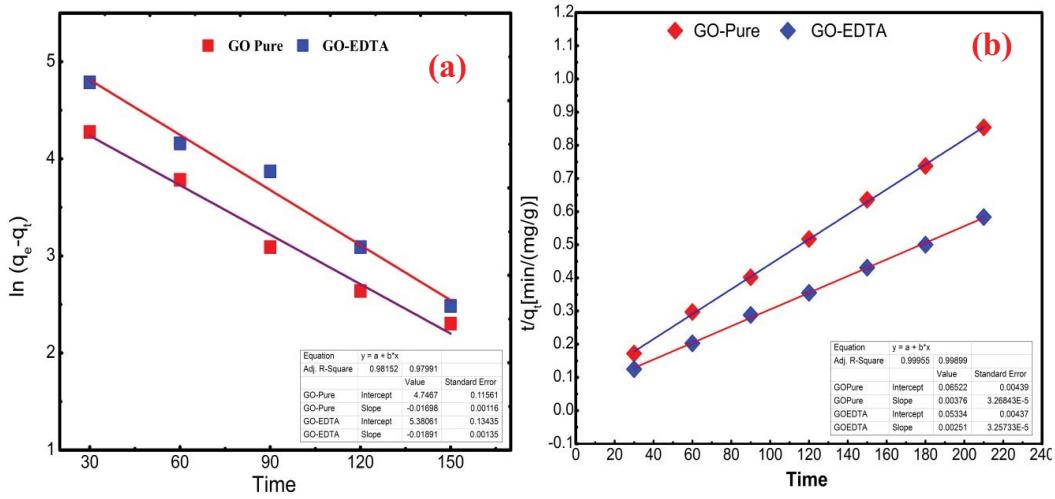

Fig. 11. (a) Pseudo-first-order kinetic and (b) pseudo-second-order kinetic for lead on to graphene oxide and graphene oxide with EDTA.

Table 3
Maximum adsorption capacity of different adsorbents for Pb(II) ions

Adsorbents	Conditions	q_{max} (mg/g)	References
Layered double hydroxides (LDHs)	pH = 5; T = 30°C	45.66	[38]
CJA porous silica material	pH = 5.5	175.16	[39]
Mesoporous material (MoCA)	pH = 5.5	206.17	[40]
Mesoporous silica (TSNT ligand)	pH = 7.5	184.32	[8]
Mesoporous conjugated adsorbent (MpCA)	pH = 5.5	192.16	[41]
Nanoscale SiO_2-Al_2O_3	pH = 6.5; T = 25°C	92.0	[12]
Graphene oxide	pH = 6.0; T = 40°C	246	This work
GO-EDTA	pH = 6.0; T = 40°C	360	This work

adsorbent was still able to remove 90% Pb. Madadrang et al. [2] found that washing acidic solutions at pH less than 2.0 desorbs 90% of the lead from EDTA-GO and GO surfaces, suggesting that GO can be reused after treatment with an HCl solution. Energy-dispersive X-ray spectroscopy was used to monitor the surface element components of EDTA-GO and GO samples before and after washing during desorption. Desorption was measured by the strength of the Pb signal at the EDTA-GO surface. Washing diminished the Pb signal, confirming desorption. HCl can remove 92% of Pb in 1 h. GO-EDTA can remove EDTA-adsorbed GO Pb(II) because it is easily desorbed. After 10 cycles, EDTA-GO maintained 80% Pb(II) elimination. Therefore, its prepared GO is regenerated and reused after being treated with an HCl solution, a comprehensive application perspective for the cost-effective removal of Pb(II) from aqueous solutions.

3.6. Adsorption mechanism of GO and GO-EDTA for the removal of Pb

Due to the fact that the GO containing various oxygen functional groups such as epoxide, carboxylic, and hydroxyl functional groups, these groups play an important role in the efficient removal of lead ions. Generally, the adsorption of cationic heavy metals such as Pb(II) on GO surfaces mainly involves the electrostatic attraction (cation-pi interaction and ionic interaction) between the opposite charges and surface complexation [37]. In the current work, the researchers functionalized GO with EDTA, a strong chelating hexadendate ligand that can bind to most of the metals, to increase the number of oxygen-containing functional groups in GO and therefore, increase the metal adsorption capacity of GO-EDTA. GO reacts with EDTA-silane, and the reaction between Si–OH and C–OH of graphene can link EDTA to the graphene surface via Si–O–C bonds. Thus, chelating groups are added to the surface of GO. Due to the formation of the amine group on EDTA, EDTA which was linked to the GO surface, this results in the formation of a basic amount of EDTA-GO. Because the number of functional groups in GO-EDTA adsorbents affects their adsorption capacity, the results show that EDTA-GO outperforms pure GO. In addition, the higher removal efficiency of Pb(II) is probably due to the higher stability constant of Pb(II)-EDTA complex (log$K$ ≈ 18.0). Pb(II) removal with EDTA-GO is achieved through two adsorption processes. The first mechanism for adsorption is an ion-exchange interaction between lead(II) and groups with either a COOH or OH group. The second mechanism of Pb(II) adsorption was surface complexation of Pb(II) with EDTA. The higher removal efficiency of Pb(II) is probably due to the higher stability constant of Pb(II)-EDTA complex (log$K$ ≈ 18.0) [2,42]. Fig. 12 presents the adsorption mechanism of Pb ions on GO and GO-EDTA surfaces in an aqueous solution as follows:

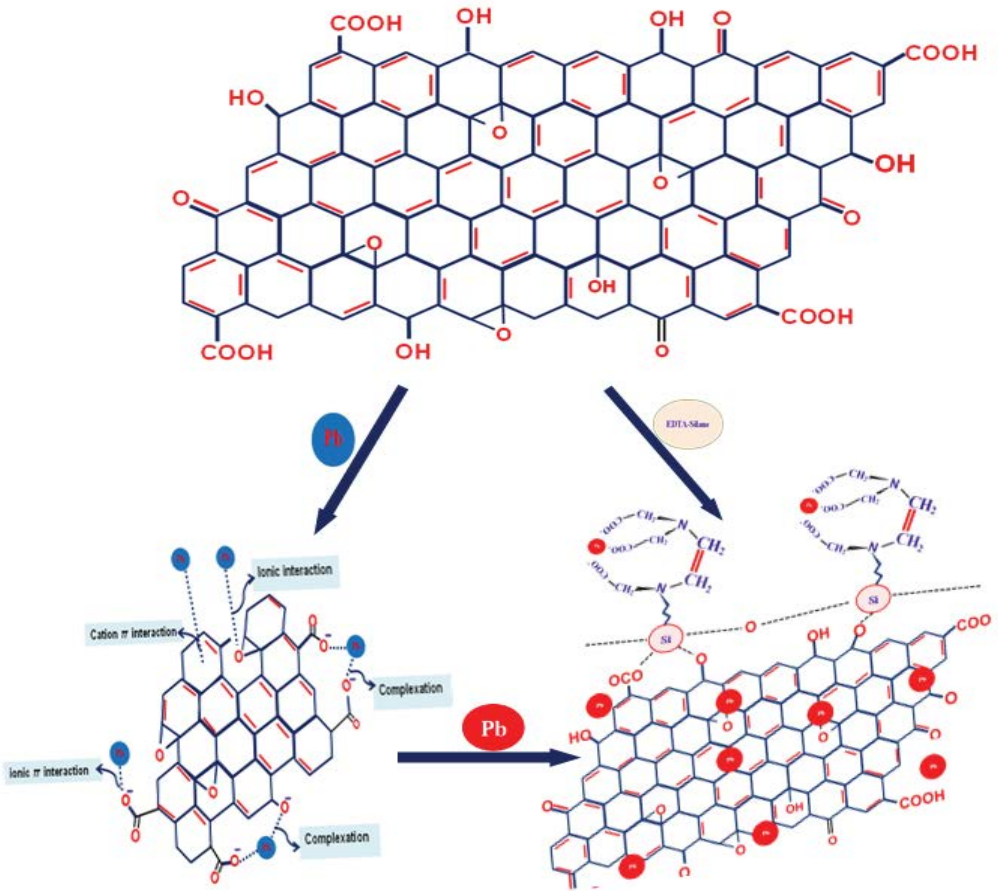

Fig. 12. Adsorption mechanism of Pb ions on GO and GO-EDTA surfaces from an aqueous solution.

- Pb(II) reacts with −COOH and −OH groups on GO surface to form a complex

$$GO - COOH + Pb^{2+} \rightarrow GO - COO^{-} - Pb^{2+} + H^{+}$$

$$(GO - COOH)_2 + Pb^{2+} \rightarrow (GO - COO^{-}) - Pb^{2+} + 2H^{+}$$

$$GO - OH + Pb^{2+} \rightarrow GO - O^{-} - Pb^{2+} + 2H^{+}$$

- Pb(II) may also react with COOH groups of EDTA to form a complex with EDTA groups

$$GO - EDTA - COOH + Pb^{2+} \rightarrow GO - EDTA - COO^{-} - Pb^{2+} + H^{+}$$

$$(GO - EDTA - COOH) + Pb^{2+} \rightarrow (GO - EDTA - COO^{-})_2 - Pb^{2+} + 2H^{+}$$

3.7. Removal of lead ions from real groundwater samples

The method used in the present work has been applied for removal of lead from real samples collected from the groundwater of a desert reach pilot area to the west of El-Mina, mid Upper Egypt. A comparison between the concentration of the lead in the samples before and after the adsorption process in this study is shown in Table 1. It was found that the removal percentage of lead from the groundwater was less than 0.008 mg/L. From the results, it can be concluded that graphene oxide functionalized with ethylene diamine tera-acetic acid was an efficient way to remove lead metals from water. Moreover, these results completely agree with the previous studies.

4. Conclusion

Graphene oxide was prepared by improved hammer method. It has been characterized using HR-TEM, FT-IR, XRD and Raman spectroscopy. The as-prepared GO was successfully funcationalized by chelating EDTA. The prepared GO and GO-EDTA was applied as adsorbent for Lead from water. It was found that funcationalization of GO with EDTA improved the removal of Pb(II). The effects of contact time, pH, and temperature on adsorption process have been investigated. The results indicated that the maximum adsorption capacity of GO for Pb(II) was about 246 while of GO-EDTA was about 360 mg/g, respectively. The results showed that pH ≈ 6 and temperature = 40°C are the best conditions for removal of Pb(II) from water. Langmuir and Freundlich isotherms were applied to describe equilibrium adsorption and the results confirmed that the equilibrium adsorption of Pb(II) are best fitted to Langmuir isotherm. Adsorption kinetics were studied by applying pseudo-first-order and pseudo-second-order on the experimental data. The adsorption of Pb(II) onto GO and GO-EDTA revealed that the pseudo-second-order model is the best represented adsorption kinetics. The developed method has been applied on real groundwater samples where the lead concentration that exceed permissible level has been removed by absorption on the prepared GO functionalized with EDTA. This result indicated that the prepared materials (GO and GO-EDTA) increased the adsorbent capacity for lead removal from ater.

References

[1] D.H.K. Reddy, S.-M. Lee, Application of magnetic chitosan composites for the removal of toxic metal and dyes from aqueous solutions, Adv. Colloid Interface Sci., 201 (2013) 68–93.
[2] C.J. Madadrang, H.Y. Kim, G. Gao, N. Wang, J. Zhu, H. Feng, M. Gorring, M.L. Kasner, S. Hou, Adsorption behavior of EDTA-graphene oxide for Pb(II) removal, ACS Appl. Mater. Interfaces, 4 (2012) 1186–1193.
[3] A. Shahat, H.M. Hassan, H.M. Azzazy, E. El-Sharkawy, H.M. Abdou, M.R. Awual, Novel hierarchical composite adsorbent for selective lead(II) ions capturing from wastewater samples, Chem. Eng. J., 332 (2018) 377–386.
[4] Md. Rabiul Awual, Md. Munjur Hasan, J. Iqbal, A. Islam, Md. Aminul Islam, A.M. Asiri, M.M. Rahman, Naked-eye lead(II) capturing from contaminated water using innovative large-pore facial composite materials, Microchem. J., 154 (2020) 104585, doi: 10.1016/j.microc.2019.104585.
[5] Md. Murshed Bhuyan, O.B. Adala, H. Okabe, Y. Hidaka, K. Hara, Selective adsorption of trivalent metal ions from multielement solution by using gamma radiation-induced pectin-acrylamide-(2-acrylamido-2-methyl-1-propanesulfonic acid) hydrogel, J. Environ. Chem. Eng., 7 (2019) 102844, doi: 10.1016/j.jece.2018.102844.
[6] D. Citak, M. Tuzen, A novel preconcentration procedure using cloud point extraction for determination of lead, cobalt and copper in water and food samples using flame atomic absorption spectrometry, Food Chem. Toxicol., 48 (2010) 1399–1404.
[7] G.A. Adebisi, Z.Z. Chowdhury, P.A. Alaba, Equilibrium, kinetic, and thermodynamic studies of lead ion and zinc ion adsorption from aqueous solution onto activated carbon prepared from palm oil mill effluent, J. Cleaner Prod., 148 (2017) 958–968.
[8] Md. Rabiul Awual, Md. Munjur Hasan, A novel fine-tuning mesoporous adsorbent for simultaneous lead(II) detection and removal from wastewater, Sens. Actuators, B, 202 (2014) 395–403.
[9] Md. Shad Salman, H. Znad, Md. Nazmul Hasan, Md. Munjur Hasan, Optimization of innovative composite sensor for Pb(II) detection and capturing from water samples, Microchem. J., 160 (2021) 105765, doi: 10.1016/j.microc.2020.105765.
[10] Md. Rabiul Awual, Assessing of lead(III) capturing from contaminated wastewater using ligand doped conjugate adsorbent, Chem. Eng. J., 289 (2016) 65–73.
[11] M.J. Amiri, R. Roohi, A. Gil, Numerical simulation of Cd(II) removal by ostrich bone ash supported nanoscale zero-valent iron in a fixed-bed column system: utilization of unsteady advection-dispersion-adsorption equation, J. Water Process Eng., 25 (2018) 1–14.
[12] M. Boroumand Jazi, M. Arshadi, M.J. Amiri, A. Gil, Kinetic and thermodynamic investigations of Pb(II) and Cd(II) adsorption on nanoscale organo-functionalized SiO_2-Al_2O_3, J. Colloid Interface Sci., 422 (2014) 16–24.
[13] M. Arshadi, A.R. Faraji, M.J. Amiri, Modification of aluminum–silicate nanoparticles by melamine-based dendrimer l-cysteine methyl esters for adsorptive characteristic of Hg(II) ions from the synthetic and *Persian Gulf* water, Chem. Eng. J., 266 (2015) 345–355.
[14] W.M.A. El Rouby, A.A. Farghali, M.A. Sadek, W.F. Khalil, Fast removal of Sr(II) from water by graphene oxide and chitosan modified graphene oxide, J. Inorg. Organomet. Polym. Mater., 28 (2018) 2336–2349.
[15] J. Zhao, W. Ren, H.-M. Cheng, Graphene sponge for efficient and repeatable adsorption and desorption of water contaminations, J. Mater. Chem., 22 (2012) 20197–20202.
[16] G. Zhao, J. Li, X. Ren, C. Chen, X. Wang, Few-layered graphene oxide nanosheets as superior sorbents for heavy metal ion pollution management, Environ. Sci. Technol., 45 (2011) 10454–10462.
[17] D.R. Dreyer, S. Park, C.W. Bielawski, R.S. Ruoff, The chemistry of graphene oxide, Chem. Soc. Rev., 39 (2010) 228–240.
[18] T.S. Sreeprasad, S.M. Maliyekkal, K.P. Lisha, T. Pradeep, Reduced graphene oxide–metal/metal oxide composites: facile synthesis and application in water purification, J. Hazard. Mater., 186 (2011) 921–931.

[19] G. Zhao, X. Ren, X. Gao, X. Tan, J. Li, C. Chen, Y. Huang, X. Wang, Removal of Pb(II) ions from aqueous solutions on few-layered graphene oxide nanosheets, Dalton Trans., 40 (2011) 10945–10952.
[20] G.K. Ramesha, A. Vijaya Kumara, H.B. Muralidhara, S. Sampath, Graphene and graphene oxide as effective adsorbents toward anionic and cationic dyes, J. Colloid Interface Sci., 361 (2011) 270–277.
[21] H. Amer, W.M. Moustafa, A.A. Farghali, W.M. El Rouby, W.F. Khalil, Efficient removal of cobalt(II) and strontium(II) metals from water using ethylene diamine tetra-acetic acid functionalized graphene oxide, J. Inorg. Gen. Chem., 643 (2017) 1776–1784.
[22] A.T. Abdel-Motagaly, W.M.A. El Rouby, S.I. El-Dek, I.M. El-Sherbiny, A.A. Farghali, Fast technique for the purification of as-prepared graphene oxide suspension, Diamond Relat. Mater., 86 (2018) 20–28.
[23] D.C. Marcano, D.V. Kosynkin, J.M. Berlin, A. Sinitskii, Z. Sun, A. Slesarev, L.B. Alemany, W. Lu, J.M. Tour, Improved synthesis of graphene oxide, ACS Nano, 4 (2010) 4806–4814.
[24] A.S. Doghish, G.S. El-Sayyad, A.-A.M. Sallam, W.F. Khalil, W.M.A. El Rouby, Graphene oxide and its nanocomposites with EDTA or chitosan induce apoptosis in MCF-7 human breast cancer, RSC Adv., 11 (2021) 29052–29064.
[25] W.F. Khalil, G.S. El-Sayyad, W.M.A. El Rouby, M.A. Sadek, A.A. Farghali, A.I. El-Batal, Graphene oxide-based nanocomposites (GO-chitosan and GO-EDTA) for outstanding antimicrobial potential against some *Candida* species and pathogenic bacteria, Int. J. Biol. Macromol., 164 (2020) 1370–1383.
[26] J. Park, S.-J. Park, S. Kim, Production of Pt nanoparticles-supported chelating group-modified graphene for direct methanol fuel cells, Res. Chem. Intermed., 40 (2014) 2509–2517.
[27] S. Hou, S. Su, M.L. Kasner, P. Shah, K. Patel, C.J. Madarang, Formation of highly stable dispersions of silane-functionalized reduced graphene oxide, Chem. Phys. Lett., 501 (2010) 68–74.
[28] M.S. Wietecha, J. Zhu, G. Gao, N. Wang, H. Feng, M.L. Gorring, M.L. Kasner, S. Hou, Platinum nanoparticles anchored on chelating group-modified graphene for methanol oxidation, J. Power Sources, 198 (2012) 30–35.
[29] M.S. Attia, G.S. El-Sayyad, M. Abd Elkodous, W.F. Khalil, M.M. Nofel, A.M. Abdelaziz, A.A. Farghali, A.I. El-Batal, W.M. El Rouby, Chitosan and EDTA conjugated graphene oxide antinematodes in Eggplant: toward improving plant immune response, Int. J. Biol. Macromol., 179 (2021) 333–344.
[30] N. Ding, Q. Cao, H. Zhao, Y. Yang, L. Zeng, Y. He, K. Xiang, G. Wang, Colorimetric assay for determination of lead(II) based on its incorporation into gold nanoparticles during their synthesis, Sensors (Basel), 10 (2010) 11144–11155.
[31] X. Wang, Z. Chen, S. Yang, Application of graphene oxides for the removal of Pb(II) ions from aqueous solutions: experimental and DFT calculation, J. Mol. Liq., 211 (2015) 957–964.
[32] X. Fan, W. Peng, Y. Li, X. Li, S. Wang, G. Zhang, F. Zhang, Deoxygenation of exfoliated graphite oxide under alkaline conditions: a green route to graphene preparation, Adv. Mater., 20 (2008) 4490–4493.
[33] X. Meng, D. Geng, J. Liu, M.N. Banis, Y. Zhang, R. Li, X. Sun, Non-aqueous approach to synthesize amorphous/crystalline metal oxide-graphene nanosheet hybrid composites, J. Phys. Chem. C, 114 (2010) 18330–18337.
[34] H. Chen, D. Shao, J. Li, X. Wang, The uptake of radionuclides from aqueous solution by poly(amidoxime) modified reduced graphene oxide, Chem. Eng. J., 254 (2014) 623–634.
[35] B.H. Hameed, D.K. Mahmoud, A.L. Ahmad, Equilibrium modeling and kinetic studies on the adsorption of basic dye by a low-cost adsorbent: coconut (*Cocos nucifera*) bunch waste, J. Hazard. Mater., 158 (2008) 65–72.
[36] Y.-S. Ho, Absorption of Heavy Metals From Waste Streams by Peat, A Thesis Submitted to the Faculty of Engineering of The University of Birmingham for the Degree of Doctor of Philosophy, University of Birmingham, 1995.
[37] Md. Golam Azam, Md. Humayun Kabir, Md. Aftab Ali Shaikh, S. Ahmed, M. Mahmud, S. Yasmin, A rapid and efficient adsorptive removal of lead from water using graphene oxide prepared from waste dry cell battery, J. Water Process Eng., 46 (2022) 102597, doi: 10.1016/j.jwpe.2022.102597.
[38] Md. Tofazzal Hossain, S. Khandaker, M. Mahbubul Bashar, A. Islam, M. Ahmed, R. Akter, A.K.D. Alsukaibi, Md. Munjur Hasan, H.M. Alshammari, Takahiro Kuba i, Md. Rabiul Awual h j k, Simultaneous toxic Cd(II) and Pb(II) encapsulation from contaminated water using Mg/Al-LDH composite materials, J. Mol. Liq., 368 (2022) 120810, doi: 10.1016/j.molliq.2022.120810.
[39] Md. Rabiul Awual, Novel conjugated hybrid material for efficient lead(II) capturing from contaminated wastewater, Mater. Sci. Eng., C, 101 (2019) 686–695.
[40] Md. Rabiul Awual, Mesoporous composite material for efficient lead(II) detection and removal from aqueous media, J. Environ. Chem. Eng., 7 (2019) 103124, doi: 10.1016/j.jece.2019.103124.
[41] Md. Rabiul Awual, A. Islam, Md. Munjur Hasan, M.M. Rahman, A.M. Asiri, Md. Abdul Khaleque, Md. Chanmiya Sheikh, Introducing an alternate conjugated material for enhanced lead(II) capturing from wastewater, J. Cleaner Prod., 224 (2019) 920–929.
[42] I.E. Mejias Carpio, J.D. Mangadlao, H.N. Nguyen, R.C. Advincula, D.F. Rodrigues, Graphene oxide functionalized with ethylenediamine triacetic acid for heavy metal adsorption and anti-microbial applications, Carbon, 77 (2014) 289–301.